

When Visual Evidence is Ambiguous: Pareidolia as a Diagnostic Probe for Vision Models

Qianpu Chen¹, Derya Soydaner¹, and Rob Saunders¹

Leiden Institute of Advanced Computer Science (LIACS), Leiden University, Leiden,
The Netherlands

Abstract. When visual evidence is ambiguous, vision models must decide whether to interpret face-like patterns as meaningful. Face pareidolia, the perception of faces in non-face objects, provides a controlled probe of this behavior. We introduce a representation-level diagnostic framework that analyzes detection, localization, uncertainty and bias across class, difficulty and emotion in face pareidolia images. Under a unified protocol, we evaluate six models spanning four representational regimes: vision–language models (VLMs; CLIP-B/32, CLIP-L/14, LLaVA-1.5-7B), pure vision classification (ViT), general object detection (YOLOv8), and face detection (RetinaFace). Our analysis reveals three mechanisms of interpretation under ambiguity. VLMs exhibit semantic overactivation, systematically pulling ambiguous non-human regions toward the *Human* concept, with LLaVA-1.5-7B producing the strongest and most confident over-calls, especially for negative emotions. ViT instead follows an uncertainty-as-abstention strategy, remaining diffuse yet largely unbiased. Detection-based models achieve low bias through conservative priors that suppress pareidolia responses even when localization is controlled. These results show that behavior under ambiguity is governed more by representational choices than score thresholds, and that uncertainty and bias are decoupled: low uncertainty can signal either safe suppression, as in detectors, or extreme over-interpretation, as in VLMs. Pareidolia therefore provides a compact diagnostic and a source of ambiguity-aware hard negatives for probing and improving the semantic robustness of vision and vision–language systems. Code will be released upon publication.

Keywords: Representation bias · Visual ambiguity · Model diagnostics

1 Introduction

Fig. 1 illustrates a scene in which two people stand in front of a wall socket. One person immediately perceives a face, while the other perceives only an ordinary object. After the first person traces two eyes and a mouth, the second person perceives the face as well. This scene illustrates *pareidolia*, a psychological phenomenon in which the visual system perceives meaningful patterns, including faces, in ambiguous stimuli. Rather than changes in the input, pareidolia reflects

differences in interpretation, offering insight into how visual systems resolve ambiguity and assign semantic meaning under uncertainty.

Why does pareidolia matter? When visual evidence is ambiguous, model responses reveal how semantic representations are structured, how uncertainty is expressed, and how prior knowledge is applied. This has direct implications for applications that must distinguish genuine faces from face-like patterns, such as medical imaging, surveillance, and content moderation. Pareidolia thus provides a compact probe of representational bias missed by standard benchmarks.

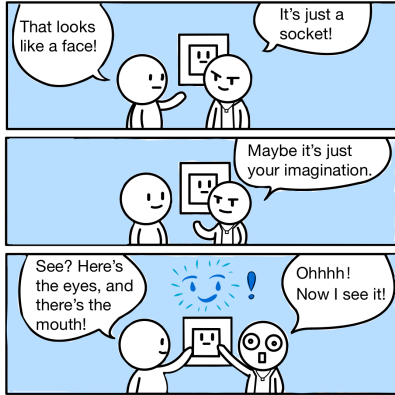


Fig. 1: Face pareidolia in an electrical outlet. The visual input is unchanged, yet observers may perceive a face, illustrating how interpretation emerges under ambiguity.

Hamilton *et al.* [5] introduced the *FacesInThings* dataset and examined face detectors on pareidolic stimuli, establishing pareidolia as a challenge. We instead treat pareidolia as a representation-level probe, using the same stimuli to analyze model responses to ambiguity, decision structure, and variation in bias and uncertainty across semantic categories, difficulty levels, and perceived emotions. This broadens the focus from face detectors to diverse representational regimes, whose responses to ambiguous face-like inputs have remained largely unexplored.

We introduce a compact diagnostic pipeline within a unified evaluation framework. Using *FacesInThings*, currently the only large-scale public dataset of human-annotated face pareidolia, we examine four representational regimes: vision-language models (contrastive VLMs: CLIP ViT-B/32 and ViT-L/14; generative VLM: LLaVA-1.5-7B), pure vision classification (ViT), general object detection (YOLOv8), and specialized face detection (RetinaFace).

- **A unified pareidolia diagnostic.** We introduce a compact evaluation suite that measures detection, localization, uncertainty and bias across class, difficulty and emotion, enabling representation-level analysis under ambiguity.
- **Cross-regime comparison under one protocol.** We apply our diagnostic to six models spanning four representation regimes, with a direct comparison.
- **Uncertainty-bias decoupling under ambiguity.** We show that predictive uncertainty is not a reliable proxy for semantic safety: high uncertainty

We observe clear differences across representational regimes. VLMs show strong semantic activation toward the human face, while ViT expresses uncertainty without directional bias. Detectors suppress pareidolic responses via strong priors, either by abstention or localization failure. Pareidolia responses are shaped not only by ambiguity, but semantic encoding and gating, and uncertainty alone does not determine bias. Our contributions are summarized below:

can coincide with low bias, while similarly low uncertainty can arise from either conservative suppression or extreme over-interpretation, establishing uncertainty and bias as distinct representational dimensions.

- **Affective and structural modulation of pareidolia.** We show that emotion selectively amplifies semantic bias in some representations, while strong architectural priors suppress pareidolia even when localization is controlled.

2 Related Work

Pareidolia and human perception. Pareidolia is used to probe how the visual system organizes ambiguous stimuli into meaningful objects [1, 17]. Face-like configurations in noise or natural scenes can trigger face-selective behavioral and neural responses, even when observers initially deny seeing a face [11]. Such effects are interpreted as evidence of priors and feature detectors rather than mere perceptual errors. Recent work asks whether neural networks exhibit analogous behavior by testing face detectors on pareidolic stimuli or examining the emergence of face-related units in models trained without explicit face supervision [5]. They typically evaluate whether models respond to pareidolia on FacesInThings dataset and how those responses compare to genuine faces. In contrast, we treat pareidolia as a structured probe and shift the focus from single-model observations to cross-regime comparison, expanding “seeing a face” to include response location, decision structure, and subgroup factors such as difficulty and emotion.

Face detection, and representation under ambiguity. Face and object detection are core computer vision tasks, with progress largely driven by benchmarks emphasizing localization accuracy [12, 15]. Detectors such as RetinaFace [3] and the YOLO family [7, 14] perform well on faces and objects. Prior work [5] focuses exclusively on face detectors, evaluating how often they respond to pareidolic faces. However, this evaluation relies on global detection metrics that capture whether a model fires but not how it localizes, allocates uncertainty, or expresses semantic bias, and it does not provide a shared diagnostic setting for comparing different model families. In parallel, VLMs such as CLIP [13] have raised concerns about calibration, bias, and behavior under ambiguity [8, 16]. Studies report systematic over-calls and semantic confusions under distribution shift or emotionally charged content [2, 6], with prompt design, calibration, and OOD detection proposed as partial remedies [9]. These analyses focus on output labels or generations, and rarely connect ambiguity to spatial behavior or controlled perceptual probes such as pareidolia. Systematic comparisons of pareidolia across model families therefore remain limited. We address this gap by evaluating face and object detectors, pure vision classification, and VLMs under a unified pareidolia-based diagnostic. Rather than proposing new architectures or losses, our approach disentangles coverage from localization, ambiguity from directional bias, and global performance from subgroup effects over hardness and emotion. This positions pareidolia as a representation-level probe of how different model families allocate probability mass to face-like inputs.



Fig. 2: Example images from the FacesInThings dataset [5]. Red bounding boxes indicate face-like regions perceived by human observers in otherwise inanimate objects.

3 Method

Our approach combines a unified diagnostic pipeline with a compact set of interpretable metrics, using pareidolic inputs not just as a benchmark but as a tool for characterizing how different models organize and express semantic evidence under ambiguity.

3.1 Task and Dataset

We use face pareidolia as a controlled probe of visual representations: when evidence is weak and ambiguous, which regions do models interpret as faces, and how do sensitivities vary across architectures and subgroups? Using images from FacesInThings (Fig. 2), we evaluate model behavior on human-annotated face-like regions. Each region is assigned to one of five coarse concepts—*Human*, *Animal*, *Cartoon*, *Alien*, or *Other*—enabling systematic comparison of bias and uncertainty under ambiguity. We do not assume a specific failure mode (e.g., over-calling *Human*); instead, pareidolia reveals how models trade off sensitivity, localization, uncertainty, and semantic preference. FacesInThings [5] is currently the only publicly available large-scale benchmark for face pareidolia, containing $\sim 5,000$ web-collected images with annotated face-like patterns. Each image includes bounding boxes for perceived pareidolic regions, a designated *primary* region (the most salient pattern), and metadata including semantic category, difficulty (*Easy/Medium/Hard*), and coarse emotion labels. We consolidate the fine-grained resemblance labels into five coarse classes to support cross-model evaluation while preserving distinctions that probe representational bias. For unified analysis across model families, we convert the annotations into a model-agnostic table where each image has consistent regions (boxes), primary flags, and coarse labels. Detection models operate on full images with outputs mapped to this table, while box-level classifiers operate directly on the annotated crops. This representation underlies all metrics and subgroup analyses in Section 4. We follow the metadata cleaning and normalization procedure from the FacesInThings demo, with minor adjustments (e.g., removing one corrupted image and enforcing consistent box and primary-region annotations).

3.2 Models and Representational Regimes

We compare how different representational regimes express pareidolia under a shared diagnostic pipeline, focusing on representational behavior rather than optimization. We evaluate six models spanning four regimes:

Vision–Language Models. CLIP ViT-B/32 and CLIP ViT-L/14 [13] are contrastive VLMs with strong semantic priors from text. We adapt them by prompting a small set of natural descriptions for each coarse class and using the resulting text embeddings as class prototypes. Each annotated region is cropped, encoded, and scored against these prototypes. This tests whether language alignment encourages particular semantic directions when visual input is ambiguous. We include LLaVA-1.5-7B [10]¹, a generative VLM that combines a vision encoder with a large language model, generating text responses. We prompt LLaVA to classify each cropped region into one of the five coarse classes, enabling direct comparison with CLIP under the same diagnostic framework.

Pure Vision Classification. To remove language entirely, we include a ViT-B/16 [4] classifier pretrained on ImageNet. We use it as a feature extractor and build prototypes in its representation space for the five coarse categories. This yields a purely visual decision rule over the same label set as CLIP, isolating the effect of semantic alignment from feature ambiguity.

General Object Detection. We use YOLOv8² as a high capacity detector trained on COCO-style data, capturing broad object-level priors. We map its category predictions into our five coarse classes (e.g., person→*Human*, animals→*Animal*) and treat detection scores as coarse-class confidence. This regime tests whether a detector that must decide both *where* and *what* to see behaves differently from box-level classifiers given the same pareidolic content.

Face-Specific Detection. RetinaFace [3] is trained to detect real human faces, providing an extreme counterpoint. Its predictions are directly mapped to the *Human* class, implementing a strong prior that we expect to suppress pareidolia at the cost of missed face-like patterns.

Despite differences, all models output the same: a set of regions with scores over the five coarse classes. This representation factors out architectural details and isolates how representational assumptions shape responses to pareidolia.

3.3 Relating Predictions to Pareidolic Regions

To jointly reason about coverage and localization, we need a clear rule for when a model “fires on” a pareidolic region. We match predicted bounding boxes to ground-truth regions using a relaxed spatial criterion: a predicted box is linked to a ground-truth region if either (1) IoU (Intersection over Union) ≥ 0.2 , or (2) the center of the predicted box falls inside the ground-truth region. We use this relaxed threshold (IoU ≥ 0.2 rather than a stricter value like 0.5) because pareidolic regions are ambiguous and models may localize them with slight offsets. Per image, we then construct a one-to-one matching by greedily pairing

¹ <https://huggingface.co/llava-hf/llava-1.5-7b-hf>

² <https://github.com/ultralytics/ultralytics>

each region with its best-matching candidate prediction (prioritizing higher IoU scores). This ensures each pareidolic region receives exactly one prediction label and each prediction is attributed to at most one region. This matching procedure separates detection failures from localization errors and ensures all subsequent metrics are defined at the level of pareidolic content rather than bounding boxes.

3.4 Core Diagnostic Metrics

We introduce a compact set of task-level metrics that factor pareidolia into detection, localization, uncertainty and bias, used throughout Section 4. Each metric is deliberately simple, but together they turn FacesInThings from a leaderboard into a diagnostic tool. We organize them into five categories, from basic coverage to higher-level semantic structure:

(1) Detection and localization. We separate overall responsiveness from spatial accuracy. For each image i with primary region r_i , the *detection rate* records whether the model produces any prediction on r_i , regardless of localization. Let $d_i = 1$ if the model produces any prediction on r_i , and 0 otherwise:

$$\text{Detection Rate} = \frac{1}{N} \sum_{i=1}^N d_i. \quad (1)$$

To capture spatial correctness, we define the *Primary Pareidolia Detection Rate (PPDR)*, which records whether the primary region has a matched prediction under a relaxed spatial rule ($\text{IoU} \geq 0.2$ or center inclusion). Let $m_i = 1$ if r_i has a matched prediction, and 0 otherwise:

$$\text{PPDR} = \frac{1}{N} \sum_{i=1}^N m_i. \quad (2)$$

Together, these metrics distinguish failure to respond from failure to localize.

(2) Difficulty-conditioned performance. FacesInThings annotates each image as *Easy*, *Medium*, or *Hard*, reflecting human perceptual difficulty. We compute detection metrics separately for each subset and examine how performance changes with increasing ambiguity.

(3) Uncertainty quantification. The *Representation Ambiguity Index (RAI)* measures how diffuse a model’s beliefs are when it responds to a pareidolic region. For each image i , we aggregate class probabilities across matched regions into a five-way distribution $p_i = (p_{i,1}, \dots, p_{i,5})$ over {Human, Animal, Cartoon, Alien, Other}, and compute its Shannon entropy:

$$H(p_i) = - \sum_{c=1}^5 p_{i,c} \log p_{i,c}. \quad (3)$$

RAI is defined as the average entropy across images:

$$\text{RAI} = \frac{1}{N} \sum_{i=1}^N H(p_i). \quad (4)$$

Low RAI indicates confident, concentrated predictions, while high RAI reflects distributed uncertainty across classes.

(4) Bias measurement. To quantify over-interpretation of pareidolic regions as *Human*, we report both box-level and image-level bias metrics. At the box level, the *False Bias Score (FBS)* measures the probability of predicting *Human* on localized non-Human regions:

$$\text{FBS} = P(\hat{y} = \text{Human} \mid y \neq \text{Human}, \text{localized}). \quad (5)$$

At the image level, we compute *non-human*→*Human* and *Alien*→*Human* rates:

$$\text{Non-human} \rightarrow \text{Human} = P(\hat{y}_{\text{primary}} = \text{Human} \mid y_{\text{image}} \neq \text{Human}), \quad (6)$$

$$\text{Alien} \rightarrow \text{Human} = P(\hat{y}_{\text{primary}} = \text{Human} \mid y_{\text{image}} = \text{Alien}), \quad (7)$$

where \hat{y}_{primary} denotes the prediction on the primary region. By conditioning on localized or primary regions, these metrics reduce confounding from pure coverage failures.

(5) GT-box-controlled evaluation metrics. To isolate semantic behavior from localization, we evaluate detectors on cropped ground-truth bounding boxes. For each box, we record whether the detector produces any *Human* detection. The *Response Rate* is defined as:

$$\text{Response Rate} = \frac{1}{M} \sum_{j=1}^M r_j, \quad (8)$$

where $r_j = 1$ if a *Human* detection is produced on box j . The *Mean Human Score* conditional on responding is:

$$\text{Mean Human Score} = \frac{1}{\sum_{j=1}^M r_j} \sum_{j=1}^M r_j \cdot s_j, \quad (9)$$

where s_j is the associated *Human* confidence. These metrics separate localization failures from semantic gating in detectors.

3.5 Evaluation Protocol

All models are evaluated on the same cleaned FacesInThings split and under the same diagnostics (Fig. 3).

Box-level models (CLIP-B/32, CLIP-L/14, LLaVA, and ViT) operate on annotated crops, while detectors (YOLOv8 and RetinaFace) operate on full images. In both cases, predictions are mapped into our common representation and matched to pareidolic regions. We use standard pretrained checkpoints without any fine-tuning on FacesInThings, so differences arise from representational choices rather than from task-specific training. All results in the following section are computed from this unified evaluation protocol.

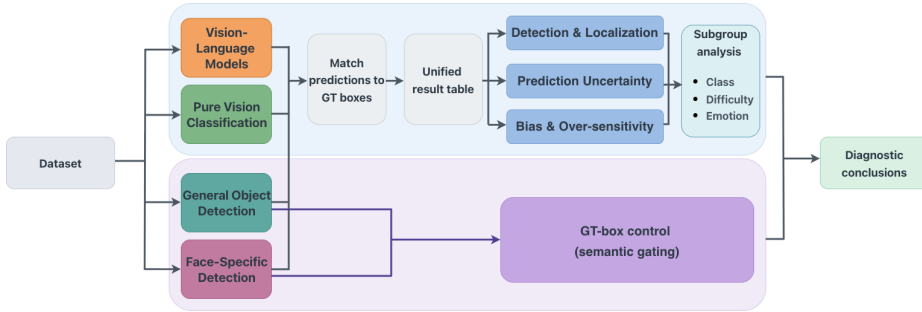


Fig. 3: Unified pareidolia diagnostic pipeline. VLMs (CLIP-B/32, CLIP-L/14, LLaVA-1.5-7B) and pure vision classifier (ViT) classify annotated regions, while general object detection (YOLOv8) and face-specific detection (RetinaFace) detect faces in full images. Predictions are mapped to a common five-class space for evaluation of detection, localization, uncertainty and bias across subgroups.

4 Experiments and Results

4.1 Detection and localization on pareidolic regions

Models differ dramatically in response frequency and localization accuracy on pareidolic regions. Box-level classifiers achieve near-perfect coverage, whereas detectors struggle with localization on ambiguous cases. We separate “any prediction” from “position-matched” detection to distinguish coverage from correct localization on pareidolic regions using the *Detection Rate* and *PPDR*, as defined in Section 3.4.

Fig. 4 and Fig. 5 shows box-level classifiers (CLIP-B/L, LLaVA, and ViT) achieve perfect scores on both metrics. YOLOv8 detects and localizes roughly 40% of pareidolic regions, missing or slightly misaligning others, with performance drops sharply on *Hard* cases. RetinaFace scores near zero on both metrics, reflecting its highly conservative real-face prior. Detection performance decreases with increasing difficulty for detectors but not for box-level classifiers. Detectors lose most ground in localization under ambiguity, whereas box-level classifiers mask localization difficulty because boxes are given.

4.2 Class confusions and aggregate bias

VLMs exhibit strong directional bias toward predicting *Human* on non-human pareidolic regions, whereas pure vision models and detectors remain more conservative, but for different reasons. We refer to such systematic *Human* predictions on non-human pareidolic regions as *over-calls*, distinguishing them from random misclassification and using them as a concrete marker of semantic overactivation.

Fig. 6 shows this pattern in terms of non-human \rightarrow *Human* and Alien \rightarrow *Human* rates. LLaVA occupies the most extreme region, with very high bias on both non-human and alien inputs. CLIP-B and CLIP-L form a secondary cluster with substantial non-human \rightarrow *Human* bias and moderate Alien \rightarrow *Human* rates. ViT sits

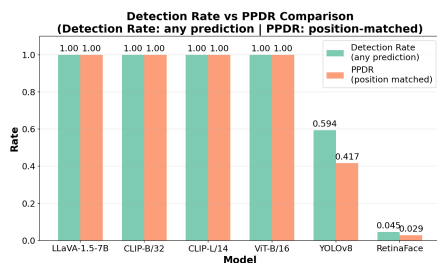


Fig. 4: Detection coverage vs. localization. Box-level classifiers saturate both metrics, while YOLOv8 and RetinaFace under-respond.

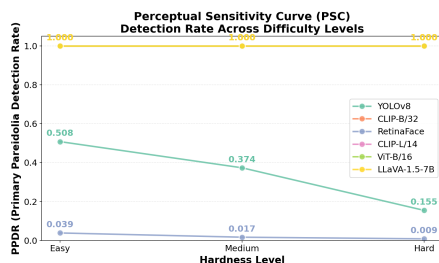


Fig. 5: Detection by difficulty. Box-level models remain stable (all curves overlap at 1.0), whereas YOLOv8 and RetinaFace decline on hard, ambiguous cases.

near the origin with low bias on both axes, reflecting high uncertainty without strong directional over-calls. YOLOv8 and RetinaFace are closest to the unbiased region, achieving low bias primarily through conservative firing and strong object- and face-centric priors. This pattern shows that language alignment systematically pulls ambiguous inputs toward the *Human* class, with LLaVA amplifying this effect, while pure vision models and detectors suppress it through either diffuse uncertainty or hard priors. The difference map between CLIP-B and CLIP-L (Fig.7) further shows that the larger model reallocates probability mass from *Human* to *Animal*, *Cartoon* and *Other* classes, softening but not eliminating the *Human* over-call. Scaling improves calibration and class separation, yet the underlying semantic prior for “human face” remains, mitigating this directional bias likely requires changing prompts, priors or training data rather than threshold tuning alone.

4.3 Uncertainty profiles and routes to low bias

Bias under ambiguity arises through different mechanisms that are not captured by confidence alone. We quantify predictive dispersion using the *Representation Ambiguity Index (RAI)*, defined as the entropy of the five-class probability distribution. As shown in Fig. 8, ViT exhibits the highest RAI while remaining nearly unbiased, reflecting an uncertainty-as-abstention behavior that avoids committing to *Human* when evidence is weak. CLIP-B and CLIP-L occupy an intermediate regime: They are less uncertain than ViT, yet they show strong directional pull toward *Human*, which is consistent with semantic overactivation rather than random uncertainty. LLaVA provides the clearest counterexample to low uncertainty as a safety signal. It produces near-deterministic predictions with very low RAI, yet it exhibits the strongest *Human* over-calls.

Detectors also exhibit low RAI, but for a different reason. Their near-zero entropy reflects hard gating driven by strong priors, not calibrated semantic uncertainty in the five-way space. This interpretation is supported by the GT-box-controlled evaluation in Section 4.5, where detectors remain conservative

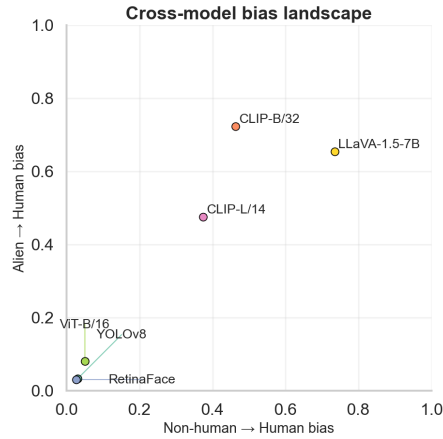


Fig. 6: Human over-call bias on pareidolic regions. Points show False Bias Score (FBS) versus non-human→Human rate, revealing stronger bias in VLMs (especially LLaVA) than in ViT, YOLOv8, and RetinaFace.

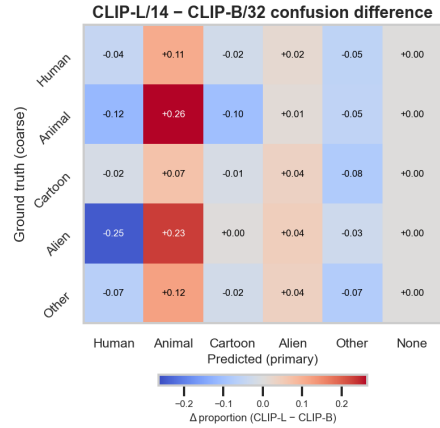


Fig. 7: Difference in prediction patterns between CLIP-B and CLIP-L. CLIP-L shifts some probability mass away from *Human* toward other non-face classes, partially reducing but not eliminating the Human over-call bias.

even when localization is factored out. Together, these results separate three routes to low or high bias under pareidolia: ViT avoids bias by remaining diffuse under ambiguity, detectors avoid bias by suppressing responses through priors, and VLMs can exhibit confident but biased interpretations that concentrate probability on *Human* even when the stimulus is non-human.

4.4 Emotion-conditioned bias and coverage

Negative emotions amplify CLIP’s *Human* over-calls, indicating that affective cues act as semantic evidence for the *Human* category. In contrast, detectors and pure vision models exhibit much weaker emotion modulation. Figure 9 shows the probability that a non-human region is predicted as *Human*. VLMs exhibit the highest bias across emotions. LLaVA shows the most extreme rates overall, while CLIP exhibits higher rates for negative emotions (e.g., scared, angry, sad) compared to happy. CLIP-L reduces the bias but preserves the same pattern, indicating that scaling softens but does not remove this effect. RetinaFace, ViT and YOLOv8 remain near zero across emotions, showing that their bias is low and far less modulated by emotion than in VLMs. Figure 10 focuses on two models that are not saturated at 100% detection. YOLOv8 varies across emotions, detecting more often on happy and unknown images, and less on angry, scared, or surprised ones, indicating that its coverage depends strongly on emotional cues. RetinaFace exhibits very low detection rates overall, with small peaks on disgusted and other categories. Detectors are therefore sensitive not only to ge-

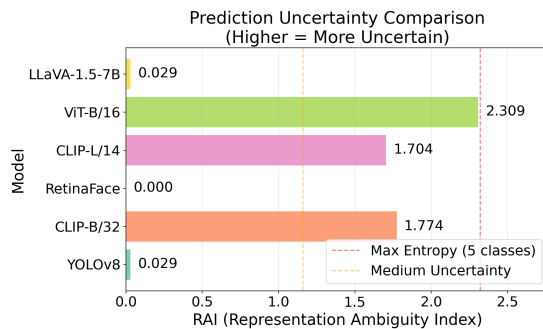


Fig. 8: Prediction uncertainty (RAI) on pareidolic regions. ViT is uncertain and unbiased, CLIP moderately uncertain and biased, LLaVA confident and strongly biased, detectors confident and conservative.

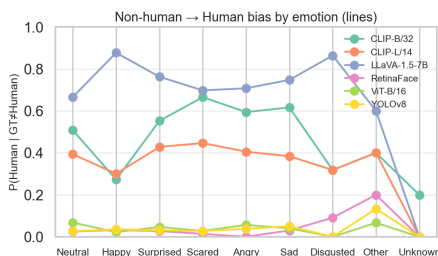


Fig. 9: Non-human→Human bias by emotion. VLMs show the highest over-call rates, with CLIP especially biased on negative emotions. ViT, YOLOv8 and RetinaFace remain near zero.

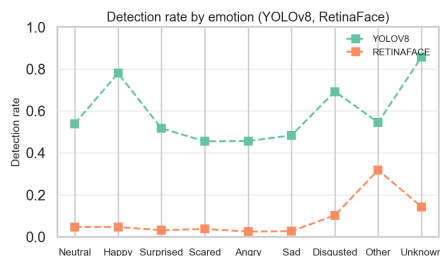


Fig. 10: Detection coverage by emotion for non-saturated models. YOLOv8 varies across emotions, while RetinaFace remains low overall.

ometry but also to coarse affective style, and that more extreme or atypical emotional cues can be more likely to trigger a face detector than neutral ones.

4.5 Detectors under GT-box-controlled evaluation

Even when localization is controlled for using ground-truth bounding boxes, detectors remain highly conservative on pareidolic regions. This confirms that their low bias stems from strong semantic priors rather than merely missed localization. The main analyses so far evaluate detectors in a full-image setting, where they must both localize and classify pareidolic regions, whereas CLIP and ViT operate directly on annotated boxes. To factor out localization and ask how detectors behave when only asked to judge a given region, we introduce a GT-box-controlled evaluation. For each FacesInThings box, we crop a padded region around the annotation and run YOLOv8 and RetinaFace on this crop, then record whether they produce any *Human* detection and with what confidence.

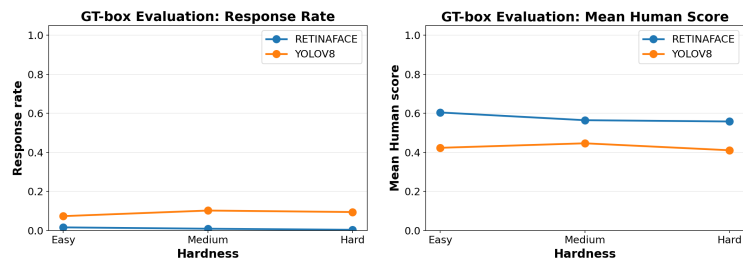


Fig. 11: GT-box-controlled detector behavior on pareidolic regions across difficulty levels. *Left:* response rate (probability of any Human detection on a GT box). *Right:* mean Human score conditional on responding.

Figure 11 shows that even when localization is controlled for using ground-truth regions, detectors remain highly conservative on pareidolic regions. The response rate (the probability that a detector produces any *Human* detection on a GT box) is low. RetinaFace fires on fewer than 2% of GT boxes on *Easy* images and even less on *Medium* and *Hard* ones. This reflects a strong prior for real faces that rarely generalizes to face-like patterns. YOLOv8 responds on roughly 7-10% of boxes depending on difficulty, far below CLIP’s near-saturated response on the same regions. When a response does occur, the mean *Human* score (the average Human confidence when the detector responds) remains relatively high for RetinaFace (≈ 0.55 to 0.60 across difficulty levels). YOLOv8’s Human scores are more moderate (≈ 0.4 to 0.45). This is consistent with strong semantic gating rather than indecision. Together with the full-image results, this control experiment confirms that low pareidolia bias in detectors is not merely a side effect of missed localization, but a consequence of their priors and decision rules.

5 Discussion

We interpret our findings through the representations and priors of each model family. GT-box analysis further clarifies that differences between model families cannot be attributed to localization alone. Pareidolia thus serves as a structured probe of probability allocation, uncertainty, and bias under ambiguity.

5.1 Uncertainty is not a reliable indicator of bias

Our results reveal that uncertainty and bias are decoupled. ViT shows that high uncertainty can protect against bias. When ViT responds to ambiguous inputs, it spreads probability across multiple classes rather than committing to one, yet it rarely misclassifies non-human patterns as *Human*. Conversely, LLaVA shows that low uncertainty does not guarantee low bias. LLaVA makes highly confident, near-deterministic predictions, yet exhibits the strongest tendency to misclassify non-human patterns as human faces among all models, far exceeding CLIP-B. Together, these findings show that responses to ambiguity are governed by semantic representations rather than their apparent confidence.

5.2 VLM architecture determines bias mechanisms

VLMs behave differently from pure vision models and detectors, but not all VLMs behave alike. Contrastive VLMs (CLIP-B and CLIP-L) show moderate uncertainty in their predictions but strong bias toward misclassifying non-human patterns as *Human*, particularly for negative emotions. This suggests that contrastive text–image alignment creates a strong human-face concept that activates easily when visual evidence is weak. LLaVA, a generative VLM, shows a fundamentally different pattern. LLaVA makes highly confident predictions with almost no uncertainty, yet exhibits the strongest bias, with the vast majority of its predictions being human faces. LLaVA’s extreme bias despite its confidence suggests that generative architectures encode even stronger face priors than contrastive ones. This difference reveals VLM design choices affect bias. Generative and contrastive training objectives produce distinct bias mechanisms. Addressing bias therefore requires architecture-specific approaches targeting prompts, pretraining data, or semantic priors, rather than simply adjusting thresholds.

5.3 Three mechanisms of bias under ambiguity

Our findings reveal three ways models handle ambiguous face-like inputs. First, detectors achieve low bias by suppressing responses: RetinaFace rarely responds to pareidolic regions due to strong face priors, while YOLOv8 maintains low bias through balanced object-class priors. When we control for localization using ground-truth bounding boxes, detectors still show low bias, indicating their behavior stems from representational priors rather than localization failures. Second, pure vision classifier achieves low bias through uncertainty: ViT spreads probability across classes rather than committing to one, avoiding systematic misclassification as *Human*. Third, VLMs show semantic overactivation with varying uncertainty: Contrastive models (CLIP) show moderate uncertainty and strong bias, while the generative model LLaVA shows very low uncertainty with even stronger bias. This three-way distinction shows that bias mechanisms depend on representational structure. The same ambiguous input can yield low bias through suppression (detectors), uncertainty (pure vision), or high bias through overactivation (VLMs), depending on how semantic concepts are encoded.

5.4 Hardness and negative emotions reveal model vulnerabilities

Hard examples degrade detector performance by reducing their ability to correctly localize pareidolic regions, pointing to localization as a key bottleneck. Emotion reveals architectural differences in how models process affective cues. For CLIP, misclassification of non-human patterns as *Human* increases under negative emotion, suggesting that affective cues act as semantic evidence for the human face concept. LLaVA shows the highest bias across all emotions, suggesting that generative VLMs may be more sensitive to affective cues than contrastive ones. Detectors maintain low bias across emotions, as priors dominate semantic associations. These patterns suggest that emotion-conditioned bias emerges from semantic alignment within different representational regimes.

These findings motivate our metric design that turns FacesInThings into a diagnostic probe rather than a leaderboard. By separating whether models respond at all from whether they localize correctly, and by examining both bias and uncertainty patterns, we distinguish localization failures from semantic ones and confident bias from cautious uncertainty. These patterns show that systematic misinterpretation under ambiguity in vision models is a structured consequence of representation and priors. Future work should consider pareidolia as a standard tool for evaluating prompts, training regimes, and calibration methods.

6 Conclusion

Face pareidolia provides a controlled ambiguity regime for examining how vision and vision-language models allocate meaning when visual evidence is weak. In contrast to standard benchmarks with clear signals, this regime reveals representational priors that are otherwise masked by strong visual evidence.

Unlike prior work that fine-tunes or optimizes specific detectors, we use pareidolia as a representation-level diagnostic across pretrained models and model families, shifting it from a performance benchmark to a probe of representation and decision structure under ambiguity.

We observe that the models cluster into three mechanisms of interpretation. VLMs exhibit semantic overactivation, systematically drawing ambiguous regions toward the *Human* concept. Pure vision classification follows an uncertainty-as-abstention route, remaining diffuse and largely unbiased. Detection-based models achieve low bias through prior-based gating, suppressing pareidolia even when localization is controlled. A central finding is that uncertainty and bias are decoupled. Low uncertainty can reflect either safe suppression, as in detectors, or extreme over-interpretation, as in generative VLM, while high uncertainty prevents directional bias, as observed in ViT. Confidence alone is thus not a reliable indicator of semantic safety under ambiguity.

Notably, increased model scale or generative alignment does not mitigate bias in this regime: the most confident model in our study exhibits the strongest directional overactivation. This has direct implications for safety-critical systems, where ambiguous face-like inputs may trigger systematic false positives that threshold tuning alone cannot fix. Instead, mitigation must address semantic directionality and alignment mechanisms.

Pareidolia highlights a path toward ambiguity-aware training. By targeting semantic overactivation rather than pixel-level perturbations, pareidolia-like inputs offer structured hard negatives that sharpen representational boundaries. More broadly, ambiguity regimes provide a stress test for how models organize meaning when evidence is insufficient, moving evaluation beyond accuracy toward the structure of semantic interpretation itself.

References

1. Caruana, N., Seymour, K.: Objects that induce face pareidolia are prioritized by the visual system. *British Journal of Psychology* **113**(2), 496–507 (2022)
2. Chefer, H., Alaluf, Y., Vinker, Y., Wolf, L., Cohen-Or, D.: Attend-and-excite: Attention-based semantic guidance for text-to-image diffusion models. *ACM transactions on Graphics (TOG)* **42**(4), 1–10 (2023)
3. Deng, J., Guo, J., Ververas, E., Kotsia, I., Zafeiriou, S.: Retinaface: Single-shot multi-level face localisation in the wild. In: *Proceedings of the IEEE/CVF conference on computer vision and pattern recognition*. pp. 5203–5212 (2020)
4. Dosovitskiy, A., et al.: An image is worth 16x16 words: Transformers for image recognition at scale. *arXiv preprint arXiv:2010.11929* (2020)
5. Hamilton, M., Stent, S., DuTell, V., Harrington, A., Corbett, J., Rosenholtz, R., Freeman, W.T.: Seeing faces in things: A model and dataset for pareidolia. In: *European conference on computer vision*. pp. 377–395. Springer (2024)
6. Huang, K., Duan, C., Sun, K., Xie, E., Li, Z., Liu, X.: T2I-CompBench++: An enhanced and comprehensive benchmark for compositional text-to-image generation. *IEEE Transactions on Pattern Analysis and Machine Intelligence* **47**(5), 3563–3579 (2025)
7. Jiang, P., Ergu, D., Liu, F., Cai, Y., Ma, B.: A review of yolo algorithm developments. *Procedia computer science* **199**, 1066–1073 (2022)
8. Lee, N., Bang, Y., Lovenia, H., Cahyawijaya, S., Dai, W., Fung, P.: Survey of social bias in vision-language models. *arXiv preprint arXiv:2309.14381* (2023)
9. Lee, T., et al.: Holistic evaluation of text-to-image models. *Advances in Neural Information Processing Systems* **36**, 69981–70011 (2023)
10. Liu, H., Li, C., Wu, Q., Lee, Y.J.: Visual instruction tuning. *Advances in neural information processing systems* **36**, 34892–34916 (2023)
11. Liu, J., Li, J., Feng, L., Li, L., Tian, J., Lee, K.: Seeing jesus in toast: neural and behavioral correlates of face pareidolia. *Cortex* **53**, 60–77 (2014)
12. Liu, L., Ouyang, W., Wang, X., Fieguth, P., Chen, J., Liu, X., Pietikäinen, M.: Deep learning for generic object detection: A survey. *International journal of computer vision* **128**(2), 261–318 (2020)
13. Radford, A., et al.: Learning transferable visual models from natural language supervision. In: *International conference on machine learning*. pp. 8748–8763. PmLR (2021)
14. Redmon, J., Divvala, S., Girshick, R., Farhadi, A.: You only look once: Unified, real-time object detection. In: *Proceedings of the IEEE conference on computer vision and pattern recognition*. pp. 779–788 (2016)
15. Russakovsky, O., et al.: Imagenet large scale visual recognition challenge. *International journal of computer vision* **115**(3), 211–252 (2015)
16. Zhou, K., Lai, E., Jiang, J.: Vlstereonet: A study of stereotypical bias in pre-trained vision-language models. In: *Proceedings of the 2nd Conference of the Asia-Pacific Chapter of the Association for Computational Linguistics and the 12th International Joint Conference on Natural Language Processing (Volume 1: Long Papers)*. pp. 527–538 (2022)
17. Zhou, L.F., Meng, M.: Do you see the “face”? individual differences in face pareidolia. *Journal of Pacific Rim Psychology* **14**, e2 (2020)